Theory of Liquid Film Growth and Wetting Instabilities on Graphene

Sanghita Sengupta,[1,2] Nathan S. Nichols,[1,2] Adrian Del Maestro,[1,2,3] and Valeri N. Kotov[1,2]
[1]Department of Physics, University of Vermont, Burlington, Vermont 05405, USA
[2]Materials Science Program, University of Vermont, Burlington, Vermont 05405, USA
[3]Institut für Theoretische Physik, Universität Leipzig, D-04103 Leipzig, Germany

(Received 2 December 2017; published 8 June 2018)

We investigate wetting phenomena near graphene within the Dzyaloshinskii-Lifshitz-Pitaevskii theory for light gases of hydrogen, helium, and nitrogen in three different geometries where graphene is either affixed to an insulating substrate, submerged or suspended. We find that the presence of graphene has a significant effect in all configurations. When placed on a substrate, the polarizability of graphene can increase the strength of the total van der Waals force by a factor of 2 near the surface, enhancing the propensity towards wetting. In a suspended geometry unique to two-dimensional materials, where graphene is able to wet on only one side, liquid film growth becomes arrested at a critical thickness, which may trigger surface instabilities and pattern formation analogous to spinodal dewetting. The existence of a mesoscopic critical film with a tunable thickness provides a platform for the study of a continuous wetting transition, as well as the engineering of custom liquid coatings. These phenomena are robust to some mechanical deformations and are also universally present in doped graphene and other two-dimensional materials, such as monolayer dichalcogenides.

DOI: 10.1103/PhysRevLett.120.236802

The wetting of an electrically neutral solid surface by a liquid is controlled by the relative size of attractive van der Waals interactions between molecules in the liquid and those between the liquid and substrate. For weak liquid-substrate interactions, the surface may undergo "partial wetting" manifested as the coexistence of distinct liquid droplets with an atomically thin layer of adsorbed molecules between them. In the opposite "complete wetting" regime, the liquid atoms are strongly attracted to the surface, resulting in the formation of a macroscopically thick film in equilibrium with the vapor above it [1].

The growth and stability of this film beyond a few atomic layers is dominated by the long-range tail of the van der Waals (vdW) interaction, which can be thought of as creating an effective repulsion between the liquid-vapor and liquid-substrate boundaries [2–4]. For intermediate liquid-surface interactions, it is possible that, at a critical film thickness d_c (larger than any atomic length scale), this repulsion vanishes and wetting is arrested due to the lack of any energetic gain for molecules in the vapor to adsorb into the liquid—a scenario known as "incomplete wetting" [1,5–7].

While a phase transition between partial and complete wetting driven by temperature is generically first order (being controlled by short-distance details of the adsorption potential), a transition from incomplete to complete wetting can be continuous due to the presence of only long-range vdW forces [8,9] (critical wetting). However, engineering substrates with weak interactions, to observe incomplete wetting and any associated critical phenomena, has been challenging, with experiments concentrating on quantum fluids at low temperatures [10,11] or liquid substrates, such as alkynes on water at high temperature [12–14].

In this Letter, we report on the physics of wetting in the novel class of geometries depicted in Fig. 1, made possible by the ability to readily fabricate and manipulate atomically flat two-dimensional (2D) crystals such as graphene [15], transition-metal dichalcogenides [16] (e.g., MoS_2), and representatives of the 2D topological insulator family [17–20] (silicene and germanene). This includes graphene placed on a substrate, submerged in a liquid, or suspended with a vacuum underneath, realizable due to the impermeability of graphene to even small atoms [21,22].

We devise an extension of the Dzyaloshinskii-Lifshitz-Pitaevskii (DLP) theory [2,3] (the standard many-body approach used for accurate analysis of experiments [23,24]) to include the polarization of a 2D material in an anisotropic layered dielectric sandwich. The results indicate that light gases near suspended 2D materials are an ideal system to study and characterize critical wetting phenomena. Our main findings include the following. (I) The presence of graphene on a substrate can enhance liquid film growth consistent with studies of its "partial wetting transparency" to liquid water [25]. (II) This effect rapidly decreases with film thickness and occurs at nanometer scales, as opposed to the micrometer distances where relativistic effects may become important [26]. (III) In the suspended geometry, the existence of vacuum beneath graphene causes incomplete wetting with a critical film thickness on the order of 2–50 nm, which can be tuned through the dynamic

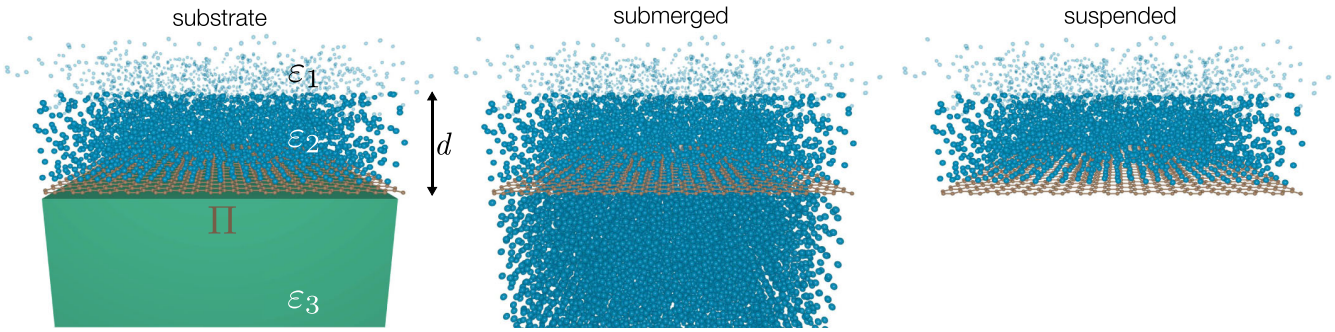

FIG. 1. Three geometries that are unique to wetting on two-dimensional materials. (Substrate) Graphene with a momentum- and frequency-dependent electronic polarization $\Pi(\boldsymbol{q}, i\omega)$ is placed on top of an insulating substrate with dielectric constant ε_3, and a macroscopic liquid film with ε_2 grows to a thickness d that is in equilibrium with its vapor ($\varepsilon_1 \approx 1$). (Submerged) Graphene is floated on top of a liquid with dielectric constant ε_2, and a liquid film of the same substance grows on the top side. (Suspended) A liquid film grows on top of a pensile graphene sheet.

polarizability of the adsorbent or the properties of the semimetal (e.g., strain). This phenomenon is universally present and can be additionally controlled in doped graphene, as well as in insulating dichalcogenides, thus spanning a wide range of 2D Dirac materials. (IV) The mesoscopic film may exhibit critical surface instabilities including pattern formation in analogy to spinodal decomposition [27–33]. Together these findings represent not only the introduction of a new platform for the study of wetting and associated critical phenomena, but hint at applications including the creation of tunable surface coating or drying mechanisms via electrostatic gating or mechanical manipulation.

The remainder of this Letter is organized as follows: we review the DLP theory and show how it is modified by the insertion of a graphene sheet. We report quantitative results for wetting and film growth in the three configurations in Fig. 1. For the suspended geometry, we examine the spreading of droplets on the liquid surface and discuss the formation of long-wavelength surface instabilities. We conclude with a discussion of the experimental measurement of these effects. Accompanying Supplemental Material provides information on the effects of temperature, different 2D materials and substrates, uniaxial strain, and electronic doping [34].

The starting point is the calculation of the vdW energy $U(d)$ of a charge neutral system composed of three substances (having dielectric functions $\varepsilon_{1,2,3}$) as shown in Fig. 1, with the atomically thin graphene layer, characterized by polarization Π, inserted at the boundary between regions 2 and 3. $U(d)$ represents the vdW interaction between the 1–2 and 2–3 material surface boundaries separated by distance d. It is well known [3,45] that $U(d)$ can be related to the momentum ($\boldsymbol{q}$) and frequency (ω) dependent effective dielectric function $\mathcal{E}(\mathbf{q}, i\omega)$, which characterizes the screening of the interlayer Coulomb potential. $U(d) = (\hbar/n)(2\pi)^{-3} \int d^2\mathbf{q} \int_0^\infty d\omega \ln \mathcal{E}(\mathbf{q}, i\omega)$, where $n = N/V$ is the density of the liquid (material 2). It should be noted that, for a single-material system (i.e., characterized by only one dielectric constant), this formula is simply the random phase approximation correlation energy, while in the case of anisotropic layered structures, it represents the fluctuation (vdW) energy. We set $\hbar = 1$ from now on.

The calculation of $\mathcal{E}$ involves the electrostatics of a three-layer system. For example, for the configurations of interest in Fig. 1, one obtains the following formula [46,47] for the properly screened interlayer Coulomb potential U_{12} between 1 and 2: $U_{12} = V_{12}/\varepsilon_g$, $V_{12} = 8\pi e^2 \varepsilon_2/[qD(q)]$, where $q = |\mathbf{q}|$ is the magnitude of the in-plane momentum,

$$D(q) = (\varepsilon_1 + \varepsilon_2)(\varepsilon_2 + \varepsilon_3)e^{qd} + (\varepsilon_1 - \varepsilon_2)(\varepsilon_2 - \varepsilon_3)e^{-qd}, \quad (1)$$

and the effect of graphene is in the additional screening characterized by

$$\varepsilon_g(\mathbf{q}, i\omega) = 1 - V_2(q)\Pi(\mathbf{q}, i\omega). \quad (2)$$

Here, V_2 is the Coulomb potential within the lower boundary plane

$$V_2 = \frac{4\pi e^2}{qD(q)}[(\varepsilon_1 + \varepsilon_2)e^{qd} + (\varepsilon_2 - \varepsilon_1)e^{-qd}]. \quad (3)$$

The polarization of graphene $\Pi(\mathbf{q}, i\omega)$ is described in the Supplemental Material [34,48]. Then, keeping in mind that $U_{12} \propto e^2 e^{-qd}/[q\mathcal{E}(\mathbf{q}, i\omega)]$, we obtain $\mathcal{E}(\mathbf{q}, i\omega) = \varepsilon_g(\mathbf{q}, i\omega)D(q)e^{-qd}$, and finally,

$$U(d) = \frac{1}{n(2\pi)^3} \int d^2\mathbf{q} \int_0^\infty d\omega \ln [\varepsilon_g(\mathbf{q}, i\omega)D(q)e^{-qd}]. \quad (4)$$

It is instructive to simplify Eq. (4) in the limit $(\varepsilon_2 - 1) \ll 1$, which is satisfied with high accuracy for the low-density systems we have studied (such as He and other light elements). In this case, their vapor can be

considered as a vacuum ($\varepsilon_1 = 1$), and suppressing $\boldsymbol{q}$ and ω dependence

$$U(d) \approx \frac{1}{n(2\pi)^3} \int d^2\mathbf{q} \int_0^\infty d\omega (\mathcal{U}_d + \mathcal{U}_g), \tag{5}$$

with dielectric

$$\mathcal{U}_d = \frac{(\varepsilon_2 - 1)(\varepsilon_3 - \varepsilon_2)}{(\varepsilon_2 + 1)(\varepsilon_3 + \varepsilon_2)} e^{-2qd} \tag{6}$$

and graphene parts

$$\mathcal{U}_g = \frac{(\frac{-4\pi e^2 \Pi}{q(\varepsilon_2+\varepsilon_3)})(\frac{\varepsilon_2-1}{\varepsilon_2+1})(\frac{2\varepsilon_2}{\varepsilon_2+\varepsilon_3})}{1 - \frac{4\pi e^2 \Pi}{q(\varepsilon_2+\varepsilon_3)}} e^{-2qd}. \tag{7}$$

The corresponding vdW force can be obtained from $F(d) = -\partial U(d)/\partial d$, which has dimensions of energy due to the normalization factors chosen in Eq. (4).

When graphene is absent ($\mathcal{U}_g = 0$), we recover the well-known DLP theory expression [2,4,49]. In particular, it describes the important property of vdW repulsion (a force per unit area known as the disjoining pressure) for $(\varepsilon_3 - \varepsilon_2) > 0$. We note that inserting graphene will always lead to repulsion as $\Pi < 0$. Equation (7) can be used to describe the three main configurations: graphene on a substrate (characterized by ε_3), submerged ($\varepsilon_3 = \varepsilon_2$), and suspended graphene ($\varepsilon_3 = 1$).

To calculate $\mathcal{U}_d$, we take the dielectric function of light elements to have a single oscillator form: $\varepsilon_2(i\omega) = 1 + C_A/[1 + (\omega/\omega_A)^2]$, where for ^{4}He we use $\omega_A = \omega_{\mathrm{He}} \approx 27$ eV and $C_{\mathrm{He}} = 0.054$. Parameters for other materials are given in the Supplemental Material [34]. The substrate dielectric function can typically be well fitted to the form [50] $\varepsilon_3(i\omega) = 1 + C_{\mathrm{IR}}/[1 + (\omega/\omega_{\mathrm{IR}})^2] + C_{\mathrm{UV}}/[1 + (\omega/\omega_{\mathrm{UV}})^2]$. For example, in the case of SiO_2 (quartz), $\omega_{\mathrm{UV}} \approx 13.37$eV, $\omega_{\mathrm{IR}} \approx 0.138$ eV, and $C_{\mathrm{IR}} = 1.93$, $C_{\mathrm{UV}} = 1.359$. Other cases are studied in the Supplemental Material [34].

The final result can be conveniently written as

$$F(d) = \frac{\omega_A}{n16\pi^2} \frac{I(d)}{d^3} \equiv \frac{\Gamma(d)}{d^3}, \tag{8}$$

where the dimensionless expression for $I(d)$ is given in the Supplemental Material [34] and is used to calculate $\Gamma(d)$. It is clear from Eqs. (5)–(7) that the dielectric part leads to a pure $1/d^3$ dependence of the force [$\Gamma(d) = \Gamma_0$, as $\varepsilon_{1,2,3}$ do not depend on momentum]. However, the graphene contribution has substantial momentum dependence [due to the polarization $\Pi(\mathbf{q}, i\omega)$] and causes a $1/d^4$ law above some length scale. The overall behavior has the scaling form (second term due to graphene)

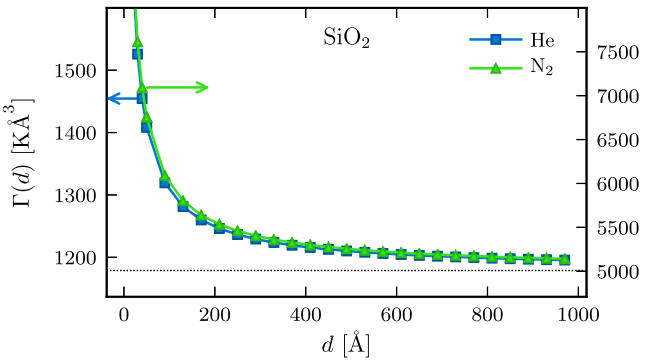

FIG. 2. Additional liquid film thickness dependence $\Gamma(d)$ (beyond $1/d^3$) of the van der Waals force between the substrate-liquid and liquid-vapor interfaces due to the insertion of graphene on a SiO_2 substrate. The dashed line represents the substrate contribution (in the absence of graphene) and a crossover from $1/d^4$ to $1/d^3$ is observed. Left vertical scale corresponds to helium and the right to nitrogen films.

$$\Gamma(d) = \Gamma_0 + \frac{\Gamma_1}{d + L}. \tag{9}$$

Figure 2 shows how the insertion of graphene on a quartz substrate enhances the vdW repulsion between the substrate-liquid and liquid-gas interfaces for helium and nitrogen gas. Graphene introduces a substantial distance dependence to the force that is larger than that previously reported for graphite [26,51]. While relativistic corrections can create crossovers in the distance dependence [26], they happen at larger micron scales, while here we see a dominant, purely nonrelativistic contribution at nanometer lengths. Similar behavior is observed for other substrates, such as 6H-SiC (see Supplemental Material [34]). The crossover length L introduced in Eq. (9) is also sensitive to the details of the substrate and for helium we find that $L \sim 10$ Å; i.e., the crossover toward pure $1/d^4$ behavior in the graphene part occurs quite rapidly.

The vdW force in the submerged and suspended geometries that are unique to 2D materials can also be evaluated with the results shown in Fig. 3 for helium, hydrogen, and nitrogen films. In all cases, we compare with calculations from Cheng and Cole [26] for adsorption on graphite (dashed lines). For submerged graphene ($\varepsilon_3 = \varepsilon_2$, filled circles), $\mathcal{U}_d = 0$ [see Eq. (6)] and $\Gamma(d)$ decays to zero, in stark contrast to the case of a graphene plated substrate. For suspended graphene ($\varepsilon_3 = 1$, squares), we observe a novel physical effect for all elements: there is a critical distance d_c at which graphene's (always positive) contribution becomes so weak it can no longer compensate the negative dielectric part and $\Gamma(d_c) = 0$. Such an effect is only possible for purely 2D materials that can be suspended without a supporting substrate—graphene [21,52,53] is the best (but not only) candidate in this family. For $d > d_c$, the liquid film growth stops under equilibrium conditions and the system becomes unstable. This is the incomplete

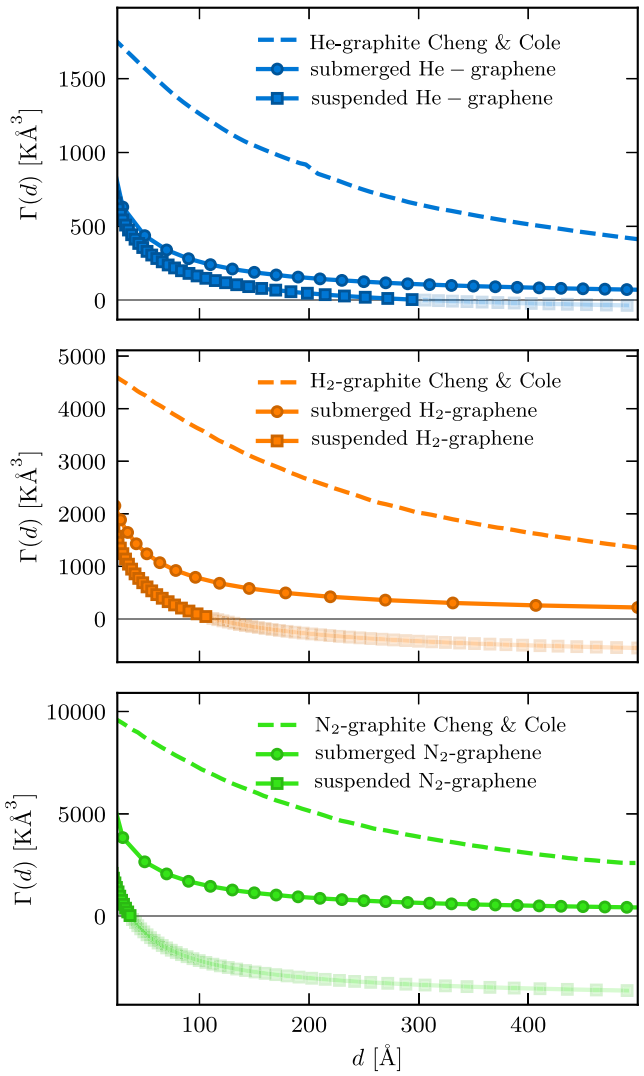

FIG. 3. Thickness dependence of the van der Waals interaction $\Gamma(d)$ for films formed on submerged and suspended graphene (see Fig. 1) composed of helium, hydrogen, and nitrogen. The dashed line corresponds to films on graphite taken from Cheng and Cole [26]. For submerged graphene, $\Gamma(d \to \infty) = 0$ and in the suspended geometry, there is an instability causing film growth to be arrested where $\Gamma(d \geq d_c) \leq 0$.

wetting scenario discussed in the Introduction. For $d < d_c$, the characteristic isotherms that determine the change of the chemical potential of the film (relative to bulk), $\Delta\mu = \mu(d) - \mu(d = \infty)$, are determined by the usual equilibrium condition (where P_0 is the saturated vapor pressure) [23,54]

$$\Delta\mu = -\frac{\Gamma(d)}{d^3} = T \ln\frac{P}{P_0}, \qquad P \leq P_0. \tag{10}$$

Figure 4 shows the resulting chemical potential for helium, hydrogen, and nitrogen on suspended graphene, which exhibits textbook behavior [54] for an unstable system. The

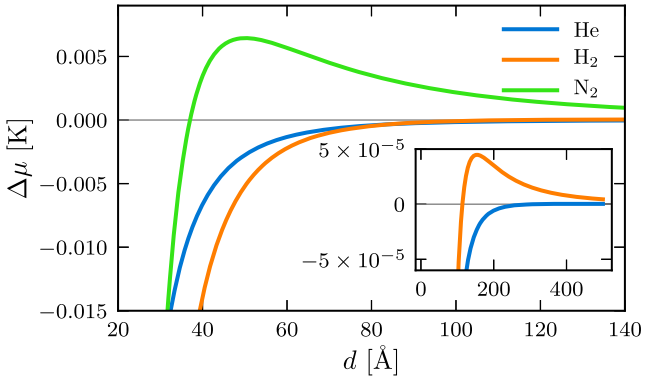

FIG. 4. Chemical potential of the liquid film (in reference to the bulk) $\Delta\mu$ as a function of distance d for suspended graphene. An instability corresponding to $\Delta\mu > 0$ is found for helium, hydrogen, and nitrogen at a finite value of $d = d_c$. (Inset) Enlarged region of the main panel showing d_c for He and H_2. Values of d_c are reported in Table I.

suspended film transitions from stable $(d < d_c)$ through a metastable region with $d > d_c$, where $\partial\Delta\mu/\partial d > 0$, and finally becomes unstable for $d > d_c$, $\partial\Delta\mu/\partial d < 0$. The values of the critical film thickness d_c are found to be on the order of 3–30 nm and are reported in Table I.

We now concentrate on the properties and implications of the incomplete wetting scenario where a liquid film with thickness d_c is absorbed on suspended graphene. As processes governing the further wetting (partial or complete) of the liquid surface are governed only by the long-range tail of the vdW interaction, they can display a wealth of phenomena of both theoretical and experimental importance [1,6,7,9,10,14,21,22,55–60]. We can formulate an important question regarding wetting of the liquid film via a calculation of the contact angle θ of droplets that can form its surface. As these droplets are "far" from the substrate, the short-range adsorption potential is irrelevant, opening up the possibility of universal and continuous critical behavior. The value of the contact angle is related to the area under the $\Delta\mu(d > d_c)$ curve [2]

$$1 - \cos(\theta) = \frac{n}{\sigma_{l-v}} \int_{d_c}^{\infty} \Delta\mu(l) dl = -\frac{n}{\sigma_{l-v}} \int_{d_c}^{\infty} \frac{\Gamma(l)}{l^3} dl, \tag{11}$$

where σ_{l-v} is the liquid-vapor surface tension. Results are shown in Table I and we find small angles on the order of a

TABLE I. Critical film thickness and contact angles for three elements. The surface tensions were taken to be $\sigma_{He} \simeq 0.26$ mN/m, $T = 2.5$ K; $\sigma_{H_2} \simeq 2$ mN/m, $T = 20$ K; $\sigma_{N_2} \simeq 10$ mN/m, $T = 70$ K.

Atom	He	H_2	N_2
d_c (Å)	300	120	35
θ (deg)	0.33	0.83	2.41

degree that increase with the polarizability of the adsorbent vapor. The fact that $\theta > 0$ in all cases allows us to consider a remarkable analogy between surface film instabilities and the theory of spinodal decomposition [27–33]. The characteristic pattern instability length scale is governed by the competition between destabilizing vdW forces and the stabilizing action of the surface tension. The wavelength λ, which corresponds to amplified surface fluctuations (which could ultimately cause "spinodal dewetting") in the unstable region ($\partial\Delta\mu/\partial d < 0$), is given by (for $d \gg L$)

$$\lambda^2 \simeq -8\pi^2 \frac{\sigma_{l-v}}{n(\frac{\partial\Delta\mu}{\partial d})} \approx \frac{8\pi^2}{3}\frac{\sigma_{l-v}d^4}{n|\Gamma_0|}. \tag{12}$$

From Fig. 3, for example, for H_2 we can estimate $|\Gamma_0| \sim 10^3$ K Å^3, which yields $\lambda \sim 10^4$–10^5 Å for $d \approx$ 150–300 Å.

In conclusion, we have considered how the relatively weak van der Waals interactions between light atoms and graphene can substantially affect their wetting behavior when graphene is placed on a substrate, submerged in a liquid or suspended above a vacuum. We find that placing graphene on a substrate enhances its propensity towards wetting during initial film growth, which may have implications for its use as a conductive coating. For suspended graphene, the absence of any substrate material leads to an instability where film growth becomes arrested at a critical thickness. As the vapor pressure above this film is increased, droplets may form, driving surface fluctuations, which can potentially have large amplitudes. It is significant that the critical film thickness d_c is dependent on mechanical deformations (e.g., uniaxial strain) in graphene and is also universally present for other 2D materials, such as members of the group-VI dichalcogenides family (MoS_2, WS_2, $MoSe_2$, etc.) [34]. Quite importantly, we also find that the instability occurs in doped graphene, within a wide range of experimentally accessible carrier densities [34]. Thus, we conclude that this is a universal phenomenon in suspended 2D Dirac materials, ranging from insulating monolayer dichalcogenides to semimetallic (undoped) and doped graphene. The exact value of d_c itself, which we find to be on the order of several hundred angstroms, depends on material characteristics, such as band gap, quasiparticle velocity, strain, and doping level. Experimental confirmation of these effects would involve the measurement of adsorbed film thickness using standard quartz microbalance [10,61] or interferometry [14] techniques. The ability to electronically or mechanically manipulate freestanding, atomically flat substrates opens up the possibility of producing an exotic quantum wetting phase transition driven by a nonthermal control parameter.

We acknowledge stimulating conversations with O. Sushkov, M. Cole, and P. Taborek on the general subject of van der Waals forces and wetting. N. N. was supported in part by the Vermont Space Grant Consortium under NASA Grant and Cooperative Agreement NNX15AP86H. A. D. acknowledges the German Science Foundation (DFG) for financial support via Grant No. RO 2247/10-1.

[1] D. Bonn, J. Eggers, J. Indekeu, and J. Meunier, Wetting and spreading, Rev. Mod. Phys. **81**, 739 (2009).
[2] I. E. Dzyaloshinskii, E. M. Lifshitz, and L. P. Pitaevskii, The general theory of van der Waals forces, Adv. Phys. **10**, 165 (1961).
[3] Y. S. Barash and V. L. Ginzburg, Electromagnetic fluctuations in matter and molecular (Van-der-Waals) forces between them, Sov. Phys. Usp. **18**, 305 (1975).
[4] I. E. Dzyaloshinskii, E. M. Lifshitz, and L. P. Pitaevskii, Van der Waals forces in liquid films, Sov. Phys. JETP **10**, 161 (1960).
[5] M. Combescot, Classification of adsorbed films, Phys. Rev. B **23**, 5623 (1981).
[6] J. G. Dash and R. Peierls, Characteristics of adsorbed films, Phys. Rev. B **25**, 5523 (1982).
[7] D. A. Huse, Incomplete wetting by adsorbed solid films, Phys. Rev. B **29**, 6985 (1984).
[8] S. Dietrich and M. Schick, Critical wetting of surfaces in systems with long-range forces, Phys. Rev. B **31**, 4718 (1985).
[9] S. Dietrich and M. Napiórkowski, Analytic results for wetting transitions in the presence of van der Waals tails, Phys. Rev. A **43**, 1861 (1991).
[10] A. D. Migone, J. Krim, J. G. Dash, and J. Suzanne, Incomplete wetting of ^{4}He films on ag and au(111) surfaces, Phys. Rev. B **31**, 7643 (1985).
[11] E. Cheng, M. W. Cole, J. Dupont-Roc, W. F. Saam, and J. Treiner, Novel wetting behavior in quantum films, Rev. Mod. Phys. **65**, 557 (1993).
[12] H. Nakanishi and M. E. Fisher, Multicriticality of Wetting, Prewetting, and Surface Transitions, Phys. Rev. Lett. **49**, 1565 (1982).
[13] E. Bertrand, D. Bonn, D. Broseta, H. Dobbs, J. O. Indekeu, J. Meunier, K. Ragil, and N. Shahidzadeh, Wetting of alkanes on water, J. Pet. Sci. Eng. **33**, 217 (2002).
[14] S. Rafaï, D. Bonn, E. Bertrand, J. Meunier, V. C. Weiss, and J. O. Indekeu, Long-Range Critical Wetting: Observation of a Critical End Point, Phys. Rev. Lett. **92**, 245701 (2004).
[15] A. H. Castro Neto, F. Guinea, N. M. R. Peres, K. S. Novoselov, and A. K. Geim, The electronic properties of graphene, Rev. Mod. Phys. **81**, 109 (2009).
[16] D. Xiao, G.-B. Liu, W. Feng, X. Xu, and W. Yao, Coupled Spin and Valley Physics in Monolayers of MoS_2 and Other Group-VI Dichalcogenides, Phys. Rev. Lett. **108**, 196802 (2012).
[17] M. Ezawa, Topological phase transition and electrically tunable diamagnetism in silicene, Eur. Phys. J. B **85**, 363 (2012).
[18] M. Ezawa, Spin-valley optical selection rule and strong circular dichroism in silicene, Phys. Rev. B **86**, 161407 (2012).

[19] N. D. Drummond, V. Zólyomi, and V. I. Falko, Electrically tunable band gap in silicene, Phys. Rev. B **85**, 075423 (2012).
[20] Z. Ni, Q. Liu, K. Tang, J. Zheng, J. Zhou, R. Qin, Z. Gao, D. Yu, and J. Lu, Tunable bandgap in silicene and germanene, Nano Lett. **12**, 113 (2012).
[21] J. Scott Bunch, S. S. Verbridge, J. S. Alden, A. M. Van Der Zande, J. M. Parpia, H. G. Craighead, and P. L. McEuen, Impermeable atomic membranes from graphene sheets, Nano Lett. **8**, 2458 (2008).
[22] R. R. Nair, H. A. Wu, P. N. Jayaram, I. V. Grigorieva, and A. K. Geim, Unimpeded permeation of water through helium-leak-tight graphene-based membranes, Science **335**, 442 (2012).
[23] E. S. Sabisky and C. H. Anderson, Verification of the Lifshitz theory of the van der Waals potential using liquid-helium films, Phys. Rev. A **7**, 790 (1973).
[24] V. Panella, R. Chiarello, and J. Krim, Adequacy of the Lifshitz Theory for Certain Thin Adsorbed Films, Phys. Rev. Lett. **76**, 3606 (1996).
[25] D. Parobek and H. Liu, Wettability of graphene, 2D Mater. **2**, 032001 (2015).
[26] E. Cheng and M. W. Cole, Retardation and many-body effects in multilayer-film adsorption, Phys. Rev. B **38**, 987 (1988).
[27] A. Sharma and R. Khanna, Pattern Formation in Unstable Thin Liquid Films, Phys. Rev. Lett. **81**, 3463 (1998).
[28] G. Reiter, A. Sharma, A. Casoli, M.-O. David, R. Khanna, and P. Auroy, Thin film instability induced by long-range forces, Langmuir **15**, 2551 (1999).
[29] A. Vrij, Possible mechanism for the spontaneous rupture of thin, free liquid films, Discuss. Faraday Soc. **42**, 23 (1966).
[30] E. Ruckenstein and R. K. Jain, Spontaneous rupture of thin liquid films, J. Chem. Soc., Faraday Trans. 2 **70**, 132 (1974).
[31] S. Herminghaus, Spinodal dewetting in liquid crystal and liquid metal films, Science **282**, 916 (1998).
[32] V. S. Mitlin, Dewetting of solid surface: Analogy with spinodal decomposition, J. Colloid Interface Sci. **156**, 491 (1993).
[33] J. S. Langer, Theory of spinodal decomposition in alloys, Ann. Phys. (N.Y.) **65**, 53 (1971).
[34] See Supplemental Material at http://link.aps.org/supplemental/10.1103/PhysRevLett.120.236802 for expanded details on the Dzyaloshinskii-Lifshitz-Pitaevskii theory, the effects of doping, different 2D materials, and temperature, which includes Refs. [35–44].
[35] S. Rauber, J. R. Klein, M. W. Cole, and L. W. Bruch, Substrate-mediated dispersion interaction between adsorbed atoms and molecules, Surf. Sci. **123**, 173 (1982).
[36] N. S. Nichols, A. Del Maestro, C. Wexler, and V. N. Kotov, Adsorption by design: Tuning atom-graphene van der Waals interactions via mechanical strain, Phys. Rev. B **93**, 205412 (2016).
[37] A. Sharma, P. Harnish, A. Sylvester, V. N. Kotov, and A. H. Castro Neto, van der Waals forces and electron-electron interactions in two strained graphene layers, Phys. Rev. B **89**, 235425 (2014).
[38] B. Amorim, A. Cortijo, F. de Juan, A. G. Grushin, F. Guinea, A. Gutiérrez-Rubio, H. Ochoa, V. Parente, R. Roldán, P. San-Jose, J. Schiefele, M. Sturla, and M. A. H. Vozmediano, Novel effects of strains in graphene and other two dimensional materials, Phys. Rep. **617**, 1 (2016).
[39] K. S. Novoselov, A. Mishchenko, A. Carvalho, and A. H. Castro Neto, 2D materials and van der Waals heterostructures, Science **353**, aac9439 (2016).
[40] V. N. Kotov, V. M. Pereira, and B. Uchoa, Polarization charge distribution in gapped graphene: Perturbation theory and exact diagonalization analysis, Phys. Rev. B **78**, 075433 (2008).
[41] D. C. Elias, R. V. Gorbachev, A. S. Mayorov, S. V. Morozov, A. A. Zhukov, P. Blake, L. A. Ponomarenko, I. V. Grigorieva, K. S. Novoselov, F. Guinea, and A. K. Geim, Dirac cones reshaped by interaction effects in suspended graphene, Nat. Phys. **8**, 172 (2012).
[42] X. Du, I. Skachko, A. Barker, and E. Andrei, Approaching ballistic transport in suspended graphene, Nat. Nanotechnol. **3**, 491 (2008).
[43] Y. Barlas, T. Pereg-Barnea, M. Polini, R. Asgari, and A. H. MacDonald, Chirality and Correlations in Graphene, Phys. Rev. Lett. **98**, 236601 (2007).
[44] G. L. Klimchitskaya and V. M. Mostepanenko, Origin of large thermal effect in the Casimir interaction between two graphene sheets, Phys. Rev. B **91**, 174501 (2015).
[45] J. N. Israelachvili, *Intermolecular and Surface Forces* (Academic Press, New York, 2011).
[46] M. I. Katsnelson, Coulomb drag in graphene single layers separated by a thin spacer, Phys. Rev. B **84**, 041407 (2011).
[47] S. M. Badalyan and F. M. Peeters, Effect of nonhomogenous dielectric background on the plasmon modes in graphene double-layer structures at finite temperatures, Phys. Rev. B **85**, 195444 (2012).
[48] V. N. Kotov, B. Uchoa, V. M. Pereira, F. Guinea, and A. H. Castro Neto, Electron-electron interactions in graphene: Current status and perspectives, Rev. Mod. Phys. **84**, 1067 (2012).
[49] E. M. Lifshitz and L. P. Pitaevskii, *Statistical Physics*, Pt. 2 (Pergamon Press, New York, 1980).
[50] L. Bergström, Hamaker constants of inorganic materials, Adv. Colloid Interface Sci. **70**, 125 (1997).
[51] J.-L. Li, J. Chun, N. S. Wingreen, R. Car, I. A. Aksay, and D. A. Saville, Use of dielectric functions in the theory of dispersion forces, Phys. Rev. B **71**, 235412 (2005).
[52] K. I. Bolotin, K. J. Sikes, Z. Jiang, M. Klima, G. Fudenberg, J. Hone, P. Kim, and H. L. Stormer, Ultrahigh electron mobility in suspended graphene, Solid State Commun. **146**, 351 (2008).
[53] J. C. Meyer, A. K. Geim, M. I. Katsnelson, K. S. Novoselov, T. J. Booth, and S. Roth, The structure of suspended graphene sheets, Nature (London) **446**, 60 (2007).
[54] L. D. Landau and E. M. Lifshitz, *Statistical Physics*, Pt. 1 (Pergamon Press, New York, 1980).
[55] P. G. De Gennes, Wetting: Statics and dynamics, Rev. Mod. Phys. **57**, 827 (1985).
[56] K. Ragil, J. Meunier, D. Broseta, J. Indekeu, and D. Bonn, Experimental Observation of Critical Wetting, Phys. Rev. Lett. **77**, 1532 (1996).
[57] F. Brochard-Wyart, J. M. di Meglio, D. Quéré, and P. G. de Gennes, Spreading of nonvolatile liquids in a continuum picture, Langmuir **7**, 335 (1991).

[58] R. Peierls, Clustering in adsorbed films, Phys. Rev. B **18**, 2013 (1978).
[59] J. G. Dash, Clustering and percolation transitions in helium and other thin films, Phys. Rev. B **15**, 3136 (1977).
[60] V. C. Weiss, E. Bertrand, S. Rafaï, J. O. Indekeu, and D. Bonn, Effective exponents in the long-range critical wetting of alkanes on aqueous substrates, Phys. Rev. E **76**, 051602 (2007).
[61] E. Van Cleve, P. Taborek, and J. E. Rutledge, Helium adsorption on lithium substrates, J. Low Temp. Phys. **150**, 1 (2008).